Supporting Information: Temperature Dependence and Energetics of Single Ions at the Aqueous Liquid-Vapor Interface

Sandeep Patel* and Shuching Ou

Department of Chemistry and Biochemistry, University of Delaware, Newark, Delaware 19716, USA

*Corresponding author. E-mail: sapatel@udel.edu

I. CONVERGENCE AND UNCERTAINTIES OF POTENTIAL OF MEAN FORCE

The convergence of PMF is shown in Figure 1 by computing PMFs of I^- at 300 K with different amount of sampling. In this figure, 2.5 ns represents the PMF is computed using 2.5 ns of production data after the initial equilibration. The inset shows the adsorption free energy as a function of sampling time. We next consider the uncertainties of the PMFs. For a potential of mean force $G(\xi)$ along a reaction coordinate ξ using umbrella sampling, we have a series of harmonic biasing potentials $K(\xi - \xi_i)^2/2$, with the reference value $G(\xi_0) = 0$. The variance in the free energy estimator is then given by the square of the cumulative statisitical error[1]:

$$\mathrm{var}[G(\xi_N)] \approx \sum_{i=1}^{N} \mathrm{var}[K\Delta\xi\bar{z}_i] \tag{1}$$

where $\bar{z}_i$ is the mean position of z in i_{th} window, which can be obtained from block averages[2]. The corresponding standard deviation $\sigma[G(\xi_N)]$ is then the square root of $\mathrm{var}[G(\xi_N)]$. In our case, $G(z = 10\ \text{Å}) = 0$, therefore the window $z = 35$ Å is expected to have the largest uncertainty. Here we plot the PMF for I^- and Cl^- along with the error bars in Figure 2. The uncertainties for the anion at bulk, GDS and the vapor phase for all temperatures used in this study are listed in Table I.

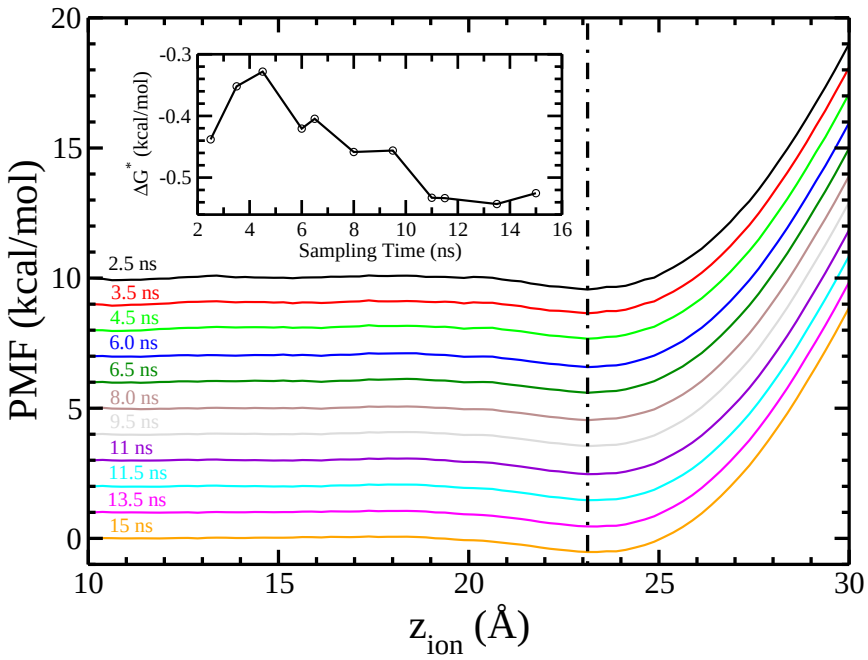

FIG. 1: PMF computed with different amount of sampling time. The inset shows the PMF minima as a function of sampling time.

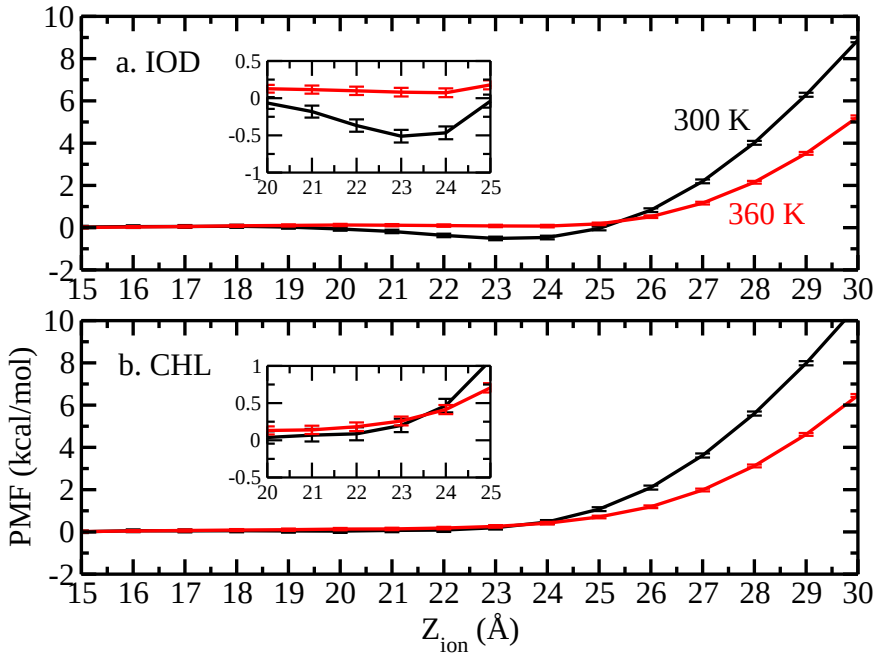

FIG. 2: Potential of mean force for single (a) iodide and (b) chloride ions across the TIP4P-FQ LV-interface at 300 K and 360 K, relative to the value at $z = 10.0$ Å, which is treat as the bulk. The inset zooms in the PMF minima along with the error bars.

System	$\sigma(z_{\text{bulk}})$	$\sigma(z_{\text{GDS}})$	$\sigma(z_{\text{vapor}})$
I^-			
280 K	0.030	0.116	0.133
300 K	0.017	0.087	0.104
320 K	0.019	0.077	0.089
340 K	0.017	0.065	0.076
360 K	0.018	0.063	0.074
Cl^-			
280 K	0.023	0.092	0.105
300 K	0.018	0.077	0.107
320 K	0.019	0.078	0.090
340 K	0.018	0.072	0.083
360 K	0.016	0.065	0.074

TABLE I: Characteristics of the uncertainties of PMF. The units are kcal/mol.

II. CONVERGENCE AND UNCERTAINTIES OF ENTHALPY

The enthalpic change $\Delta H(z)$ is computed by the difference between the average potential energy of two states. In this section we show the time profile of potential energy at certain sampling windows and the corresponding uncertainties (which are obtained by the block method) in Figure 3 and Figure 4. At the sampling time of 15 ns, the uncertainties for all the windows are less than 1 kcal/mol, which means the uncertainties of difference between two windows are less than 2 kcal/mol. This indicates that the negative enthalpic difference of I^- ($\approx$ -3 kcal/mol) in our main text is valid.

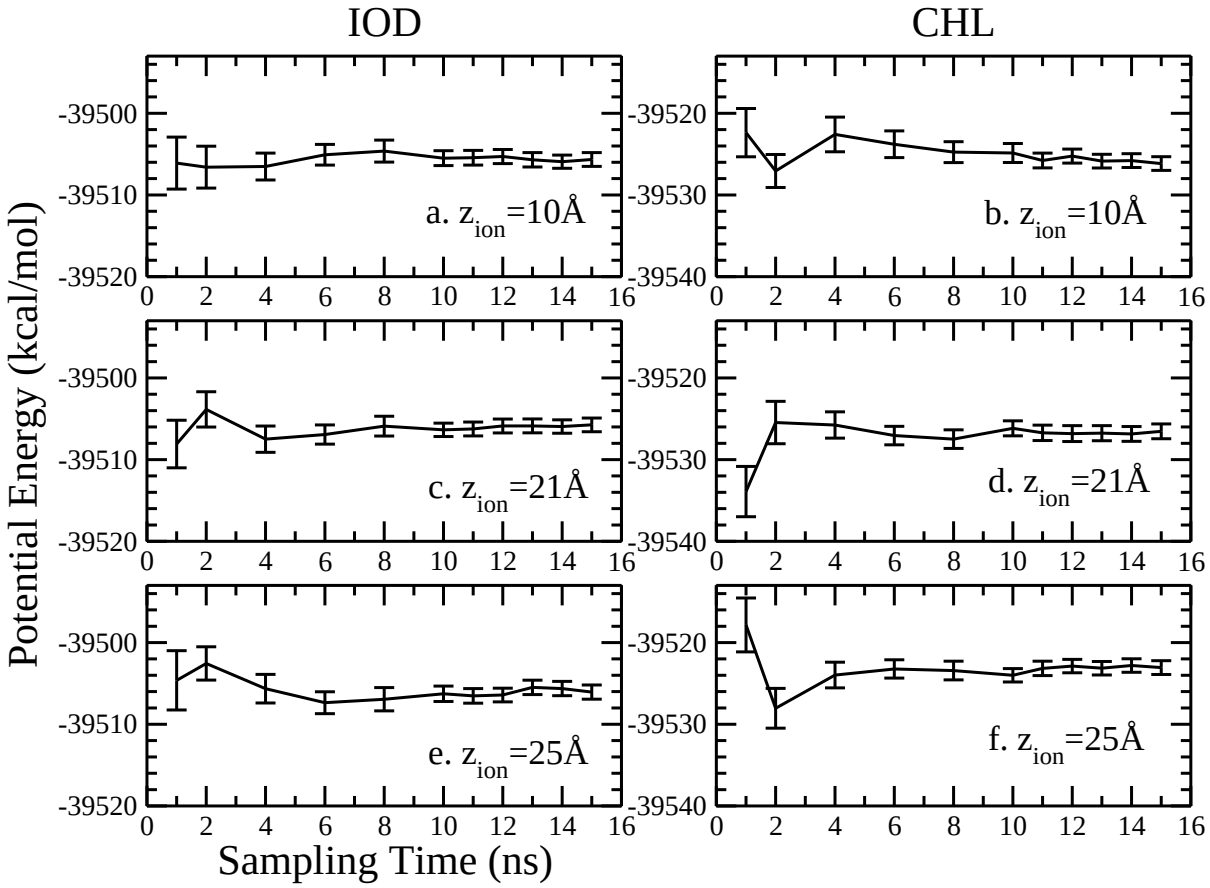

FIG. 3: Average total potential energy as a function of sampling time.

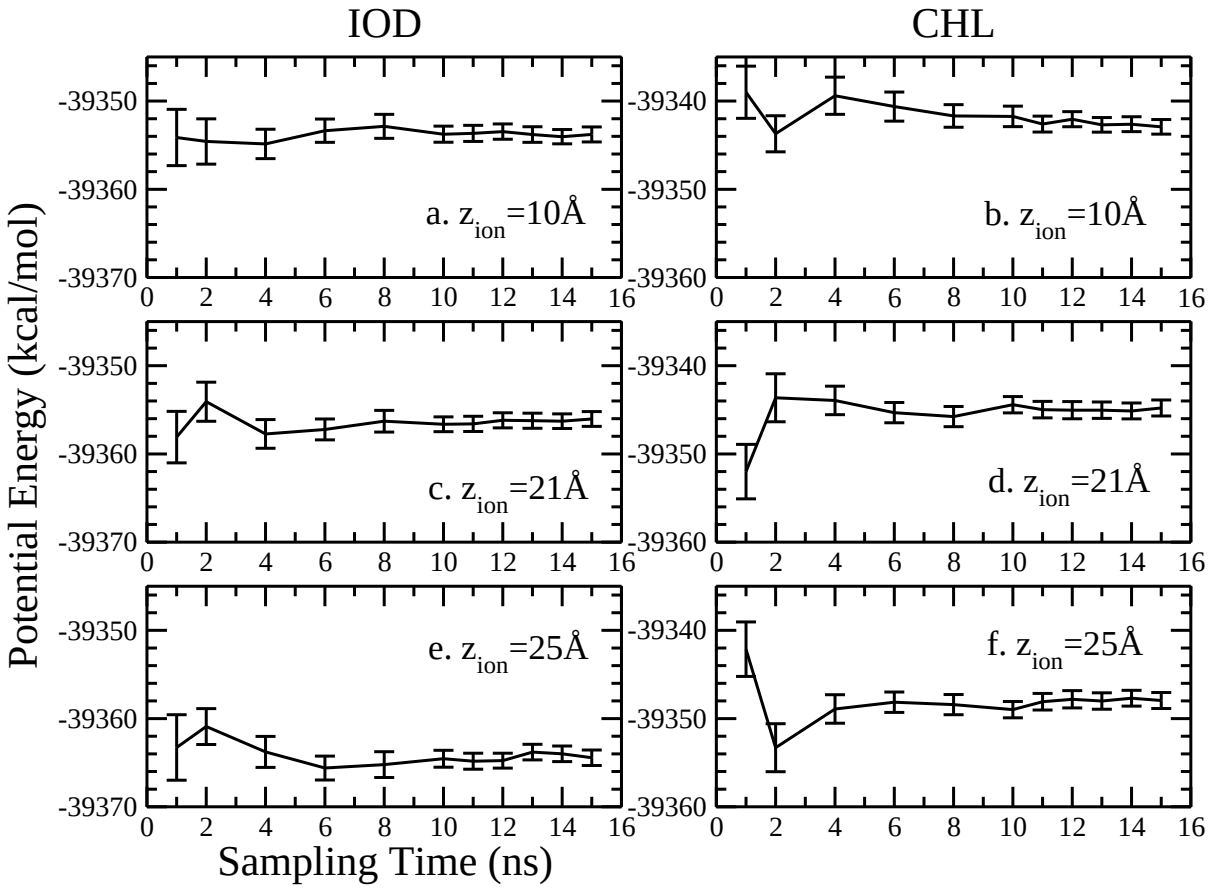

FIG. 4: Average water-water potential energy as a function of sampling time.

III. INTERACTION MAP: WATER-WATER AND ION-WATER INTERACTION

In the main text we mention that $\bar{\varepsilon}_{\mathrm{coor}}$ and $\bar{\varepsilon}_{\mathrm{L-V}}$ are both larger than $\bar{\varepsilon}_{\mathrm{bulk}}$. Here we address this with the interaction map of water (relative to the position of I^-) with all the other water molecules, as shown in Figure 5.

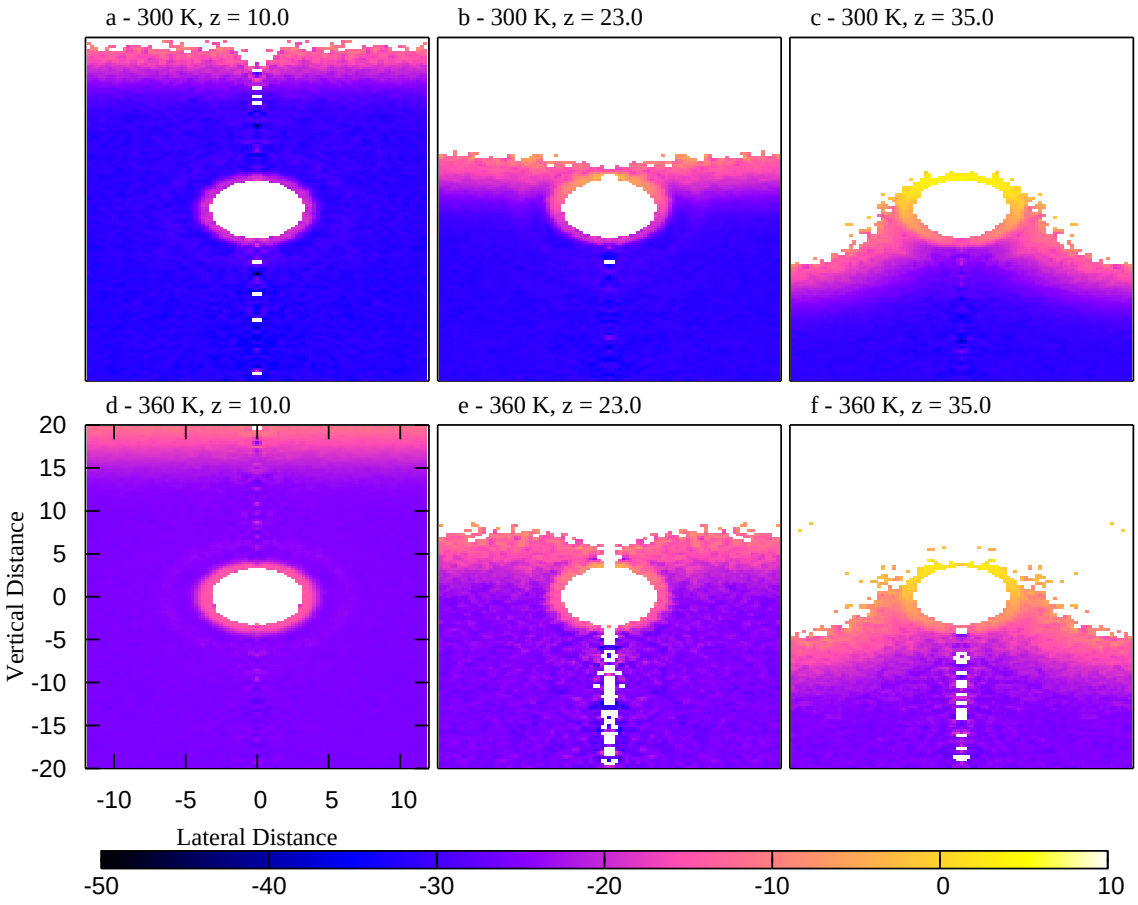

FIG. 5: (a) Interaction energy between water molecule (at position (r, z) which is relative to the position of I^-) and all the other molecules. x-axis refers to the perpendicular distance from the ion, while y-axis indicates the vertical distance. Both units are in Å. The unit for energies is kcal/mol. Panel (b) and (c) show the similar profiles with ion restraining at 23 Å and 35 Å at 300 K. Panel (d)-(f) correspond to the case of I^- at 360 K.

We plot the ion-water density map with the same convention, with further decompose the ion-water interaction into electrostatic and van der Waals interactions, as shown in Figure 6. Although the force can be quite long-ranged, the effect of ion-water interaction is majorly determined by the water molecules within 5 Å from the ion.

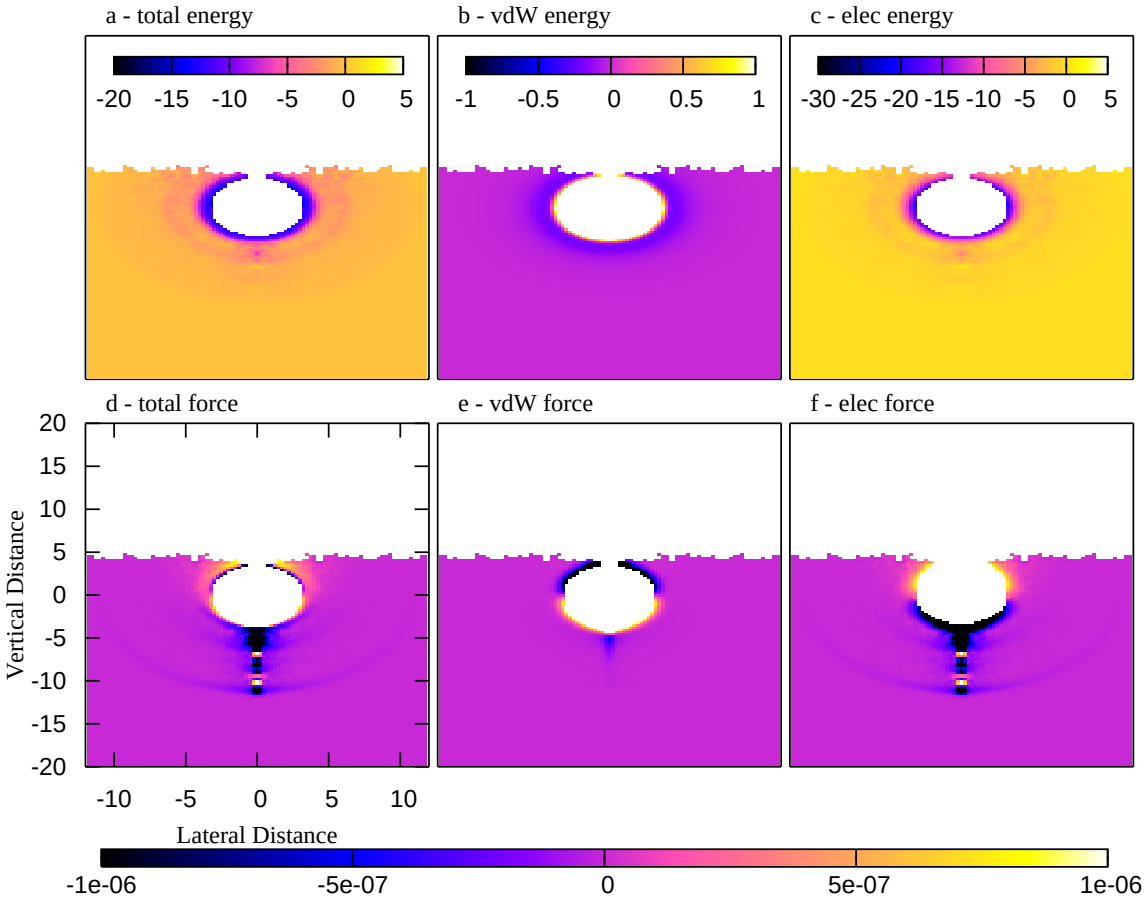

FIG. 6: (a) Interaction energy between iodide and water molecule at position (r, z) relative to the anion (which is restrained at z = 23.0 Å) and the corresponding force (panel d) at 300 K. x-axis refers to the perpendicular distance from the ion, while y-axis indicates the vertical distance. Both units are in Å. Panel (b) and (c) show the van der Waals and electrostatic contribution to the interaction energy, with (e) and (f) the corresponding forces to the anion. The unit for energies is kcal/mol, while the unit for forces is kcal/mol/Å. The favorable forces toward the liquid-vapor interface correspond to positive values (bright color), while the negative values (dark color) represent repulsive forces to the interface.

IV. SOLVATION STRUCTURE OF ANION

In the main text we mentioned the less anisotropic solvation structure of I^- rather than Cl^-. In Figure 7 and Figure 8 we show the water oxygen density relative to the position of anions. For detailed discussion of this anisotropy, please refer to Ref[3].

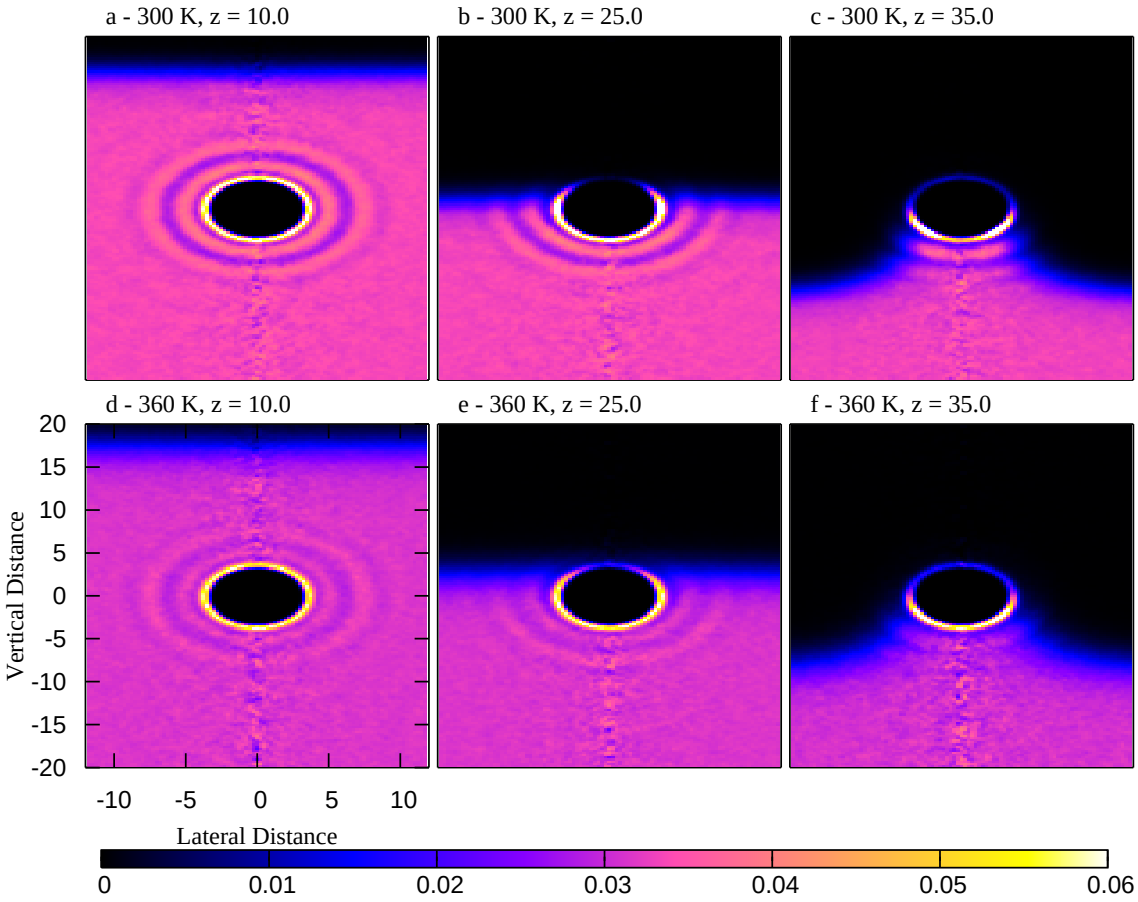

FIG. 7: Density map of water oxygen relative to I^- at 300 K and 360 K.

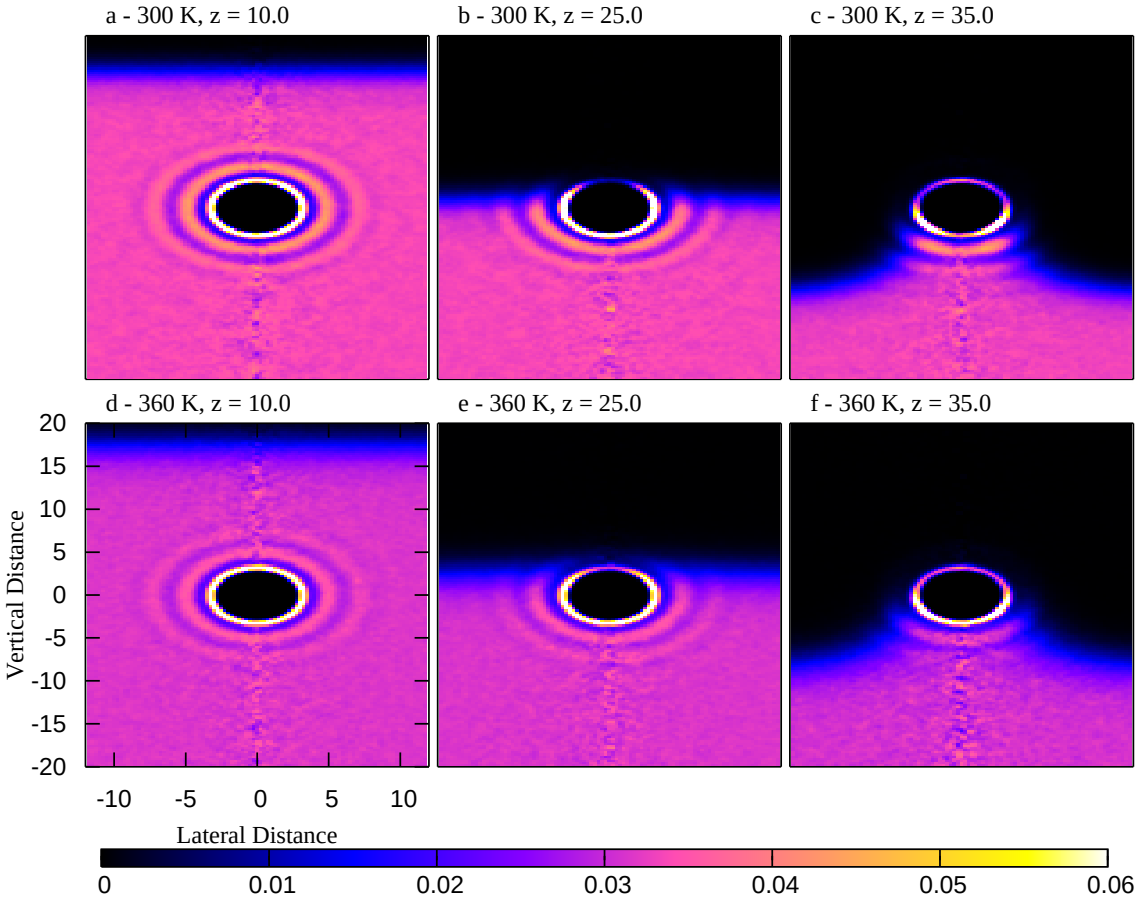

FIG. 8: Density map of water oxygen relative to Cl^- at 300 K and 360 K.

V. DISTRIBUTION OF SURFACE HEIGHT FUNCTION

Here we address that the surface height function (δh) is normally distributed regardless the ion position, as shown in Figure 9. We picked the window of I^- restrained at $z = 15$ Å as an example (displayed in inset, grey solid line) and the fitting result of Gaussian distribution(black dotted line). The form of the Gaussian distribution is:

$$g(x) = \frac{a}{\sqrt{2\pi\sigma^2}} exp \frac{-(x-\mu)^2}{2\sigma^2} \tag{2}$$

where μ is the expected value, σ^2 is the variance, σ is the standard deviation. The fitting results: $\sigma = 0.7369$ ($\pm$ 0.0002), $\mu = 0.0078$ ($\pm$ 0.0002), $a = 0.9965$ ($\pm$ 0.0003).

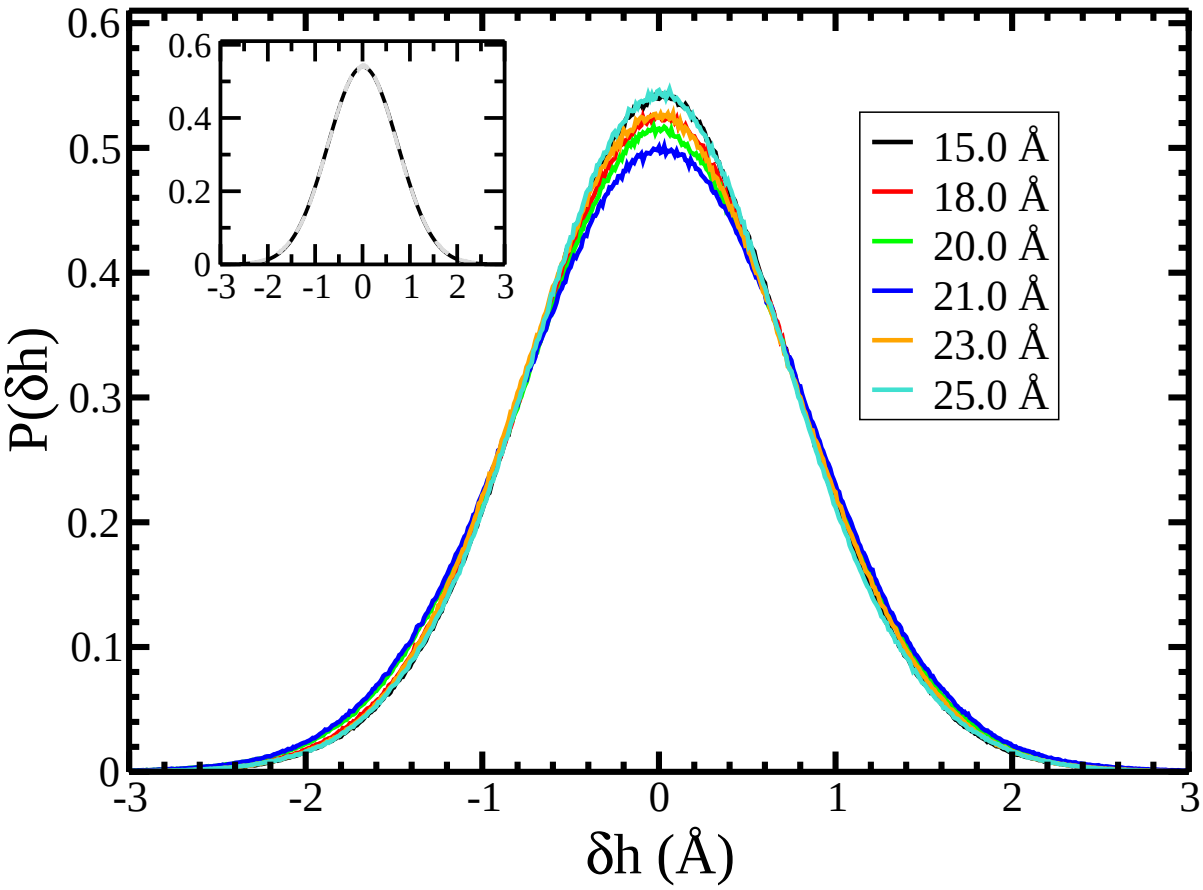

FIG. 9: Distribution of δh for different I^- positions. The inset shows an example of the fitting result of I^- restrained at $z = 15$ Å with the Gaussian distribution function.

VI. FLUCTUATIONS FOR SURFACE HEIGHT

In this section we show the general properties of surface height and normalized fluctuations (defined in the main text) at different ion-restrained windows. Shown in Figure 10a is an example of the instantaneous L-V interface for pure water with 988 TIP4P-FQ water molecules at 300 K. With sufficient sampling, we can average these instantaneous surfaces ($h_{\rm t}(x,y)$, at time t) and get the mean surface $\langle h(x,y)\rangle$ (as displayed in Figure 10b). By subtracting the mean values from the $h_{\rm t}(x,y)$, we get $\delta h_{\rm t}(x,y)$ and the height fluctuations $\delta h_{\rm t}^2(x,y)$. Notice that from our construction $\langle \delta h(x,y)\rangle = 0$. The average of surface height ($\langle\langle \delta h(x,y)\rangle\rangle$) and height fluctuation ($\langle\langle \delta h^2(x,y)\rangle\rangle$) are presented in Figure 10c and d, respectively.

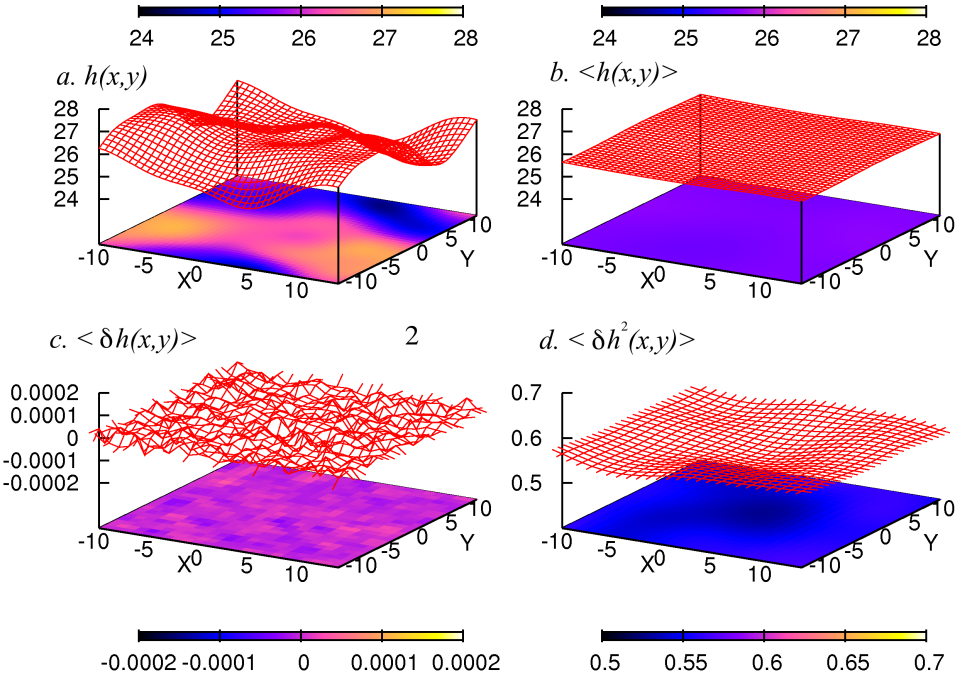

FIG. 10: Illustration of (a) instantaneous surface (b) mean surface (c) average surface height (d) average height fluctuations.

From Figure 10 we can see that the average surface is around 25.6 Å and the average height fluctuation ($\langle\langle \delta h^2(x,y)\rangle\rangle$) is about 0.56 (at 300 K). For 280 K, 320 K, 340 K and 360 K, the $\langle \delta h^2(x,y)\rangle$ for pure water are 0.50, 0.67, 0.80 and 0.95, respectively. In order to make comparison between the presence of ion and pure water case, we always shift the x and y positive of atoms when we compute the instantaneous surface, such that $\vec{r}_{xy,ion} = (0,0)$. In Figure 11 and

Figure 12 we show the $\langle h(x,y)\rangle$ and $\langle \delta h^2(x,y)\rangle$ for I^-/Cl^- at the position 10.0/25.0 Å, respectively.

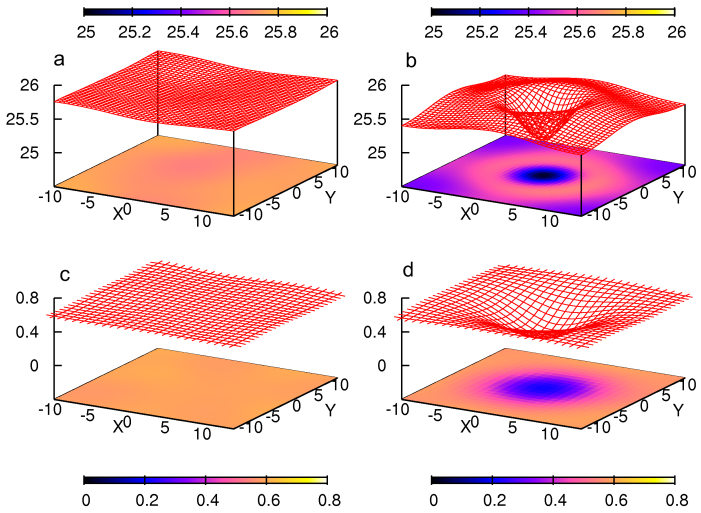

FIG. 11: Mean surface for I^- at (a) 10.0 Å (b) 25.0 Å. Average height fluctuations for I^- at (c) 10.0 Å (d) 25.0 Å.

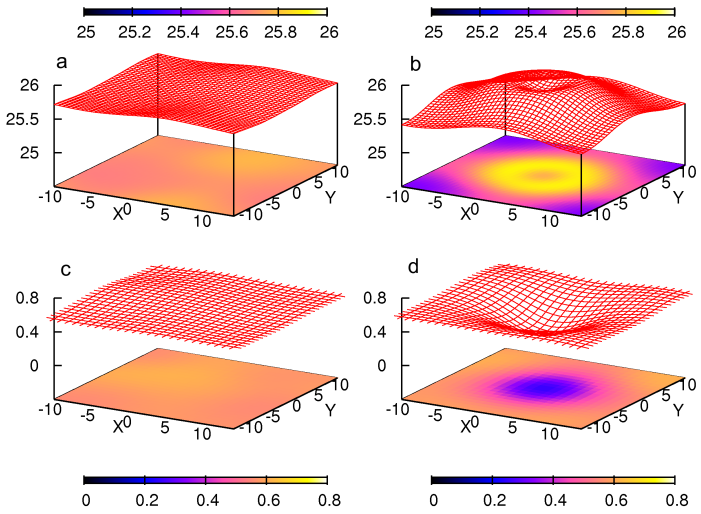

FIG. 12: Mean surface for Cl^- at (a) 10.0 Å (b) 25.0 Å. Average height fluctuations for Cl^- at (c) 10.0 Å (d) 25.0 Å.

In the main text we use surface height function and construct the covariance matrix to estimate the surface entropy, which is determined by the fineness of the resolution. As mentioned in the text, we compute the entropy every 50 ps, and the time profile is shown in Figure 15.

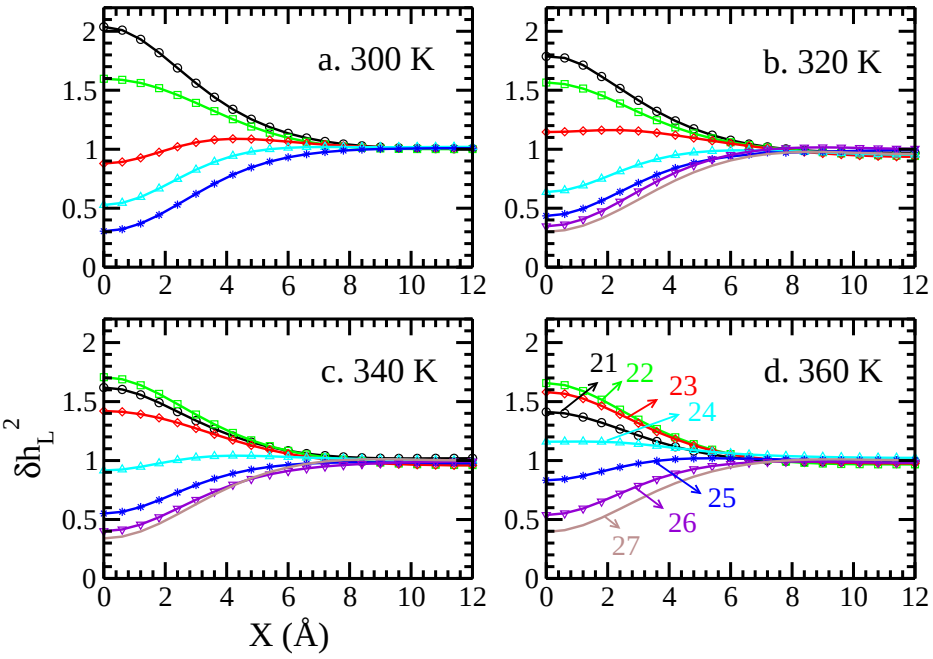

FIG. 13: Normalized surface height fluctuations, as functions of lateral displacement X (when the other lateral displacement Y is zero), for I^- at (a) 300 K (b) 320 K, (c) 340 K and (d) 360 K.

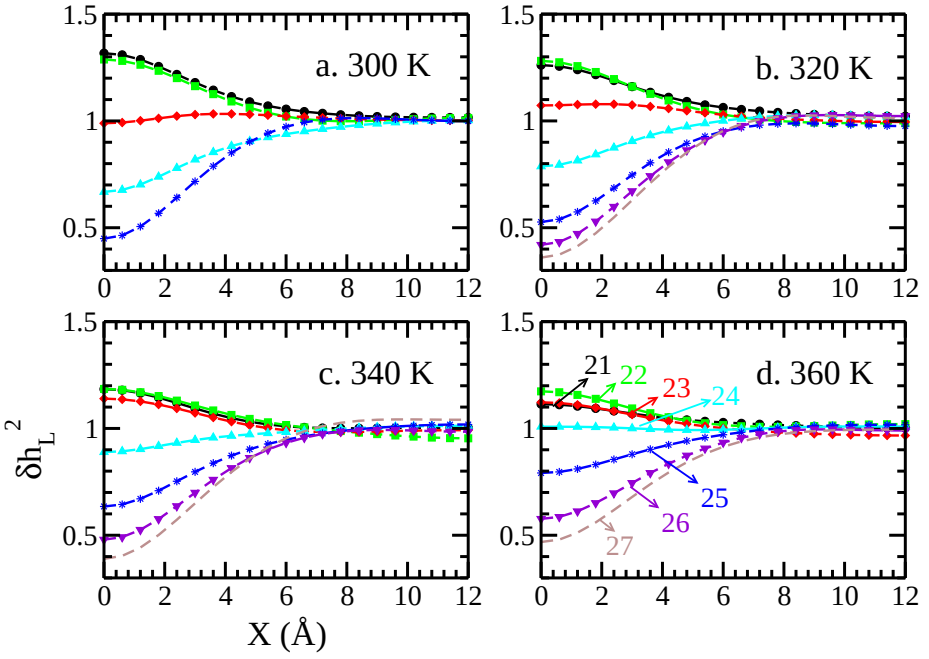

FIG. 14: Normalized surface height fluctuations, as functions of lateral displacement X (when the other lateral displacement Y is zero), for Cl^- at (a) 300 K (b) 320 K, (c) 340 K and (d) 360 K.

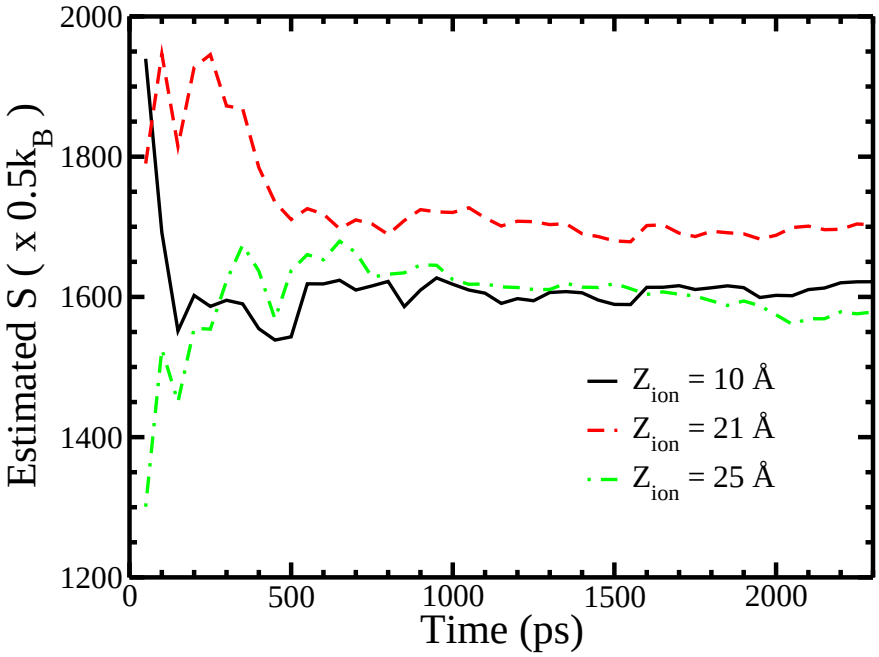

FIG. 15: Time profile of the estimated entropy.

VII. PROPERTIES OF WATER IN THE VICINITY OF ION

In the manuscript we mentioned that the mean surface for I^- is within its first hydration shell, while that of Cl^- is outside its first hydration shell. From the discussion in the main text, we already know that it is necessary to consider the water molecules above the ion. Therefore, we restrict the sampling of water above the anion for the following study of water structures. All the profiles shown in the following figures are scaled with the corresponding bulk properties, which are listed in Table II.

System	$\langle N_{\rm HB}\rangle$	$S_{\rm g}$	$\langle\mu\rangle$
280 K	3.285	0.109	2.679
300 K	3.169	0.117	2.616
320 K	3.049	0.124	2.563
340 K	2.927	0.130	2.518
360 K	2.797	0.136	2.478

TABLE II: Average number of hydrogen bond per water molecule, tetrahedral order parameter and magnitude of water dipole moment in the bulk. The unit of dipole moment is Debye.

Two water molecules were considered hydrogen bonded if the oxygen-oxygen distance is less than 3.5 Å and the $HO\cdots O$ angle is less than $30°$.[4] The average numbers of hydrogen bonding per water molecule as functions of r are shown in Figure 16.

Order parameters specific for tetrahedral configurations are of special interest for studying liquid water. The four nearest neighbors of each water molecule approximate to four vertices of a tetrahedron, because of the relative orientations of the O-H bonds and the lone pairs. These bonds and lone pairs are responsible for hydrogen bonding, which is important for the structure of liquid water. We therefore apply the tetrahedral parameter introduced by Chau et al[5] to describe the configurations of water near the anion. For a tetrahedral configuration there are five points: the four vertices of the tetrahedron and the center. In a tetrahedral arrangement, all the angles between bonds are the same, and the cosine of this angle is $-1/3$. Therefore for a water molecule, we find its closest four water molecules and define

$$S_{\rm g} = \frac{3}{32}\sum_{j=1}^{3}\sum_{k=j+1}^{4}(cos\psi_{j,k}+\frac{1}{3})^2 \tag{3}$$

where $\psi_{j,k}$ is the angle subtended at the central water between the j_{th} and k_{th} bonds. The factor of $3/32$ normalizes $S_{\rm g}$ to the range $0 < S_{\rm g} < 1$. The squaring ensures the contribution from each inter-bond angle is always greater

than or equal to zero. Hence S_g, which is the sum of the contributions from the six angles, is zero if and only if the cosines of all the angles are $-1/3$, i.e., the bonds are arranged perfectly tetrahedrally. In the case of bulk water, $S_g \approx 0.12$. The average value of $\langle S_g \rangle$ for randomly arranged bonds, with uncorrelated uniform angular distributions, is 1/4. The average values of S_g near the anions are shown in Figure 17 as functions of r. For water molecules in the first hydration shell, they have less tendency to form tetrahedral configurations. Since I^- has a larger size than Cl^-, this effect is even enhanced. As the ion approaches the L-V interface, $\langle S_g \rangle$ starts to increase, since more and more L-V interfacial water molecules are involved. These interfacial water molecules, due to the orientational preference near the L-V interface, are having more difficult to form hydrogen bonds with each other, consequently less tetrahedral co

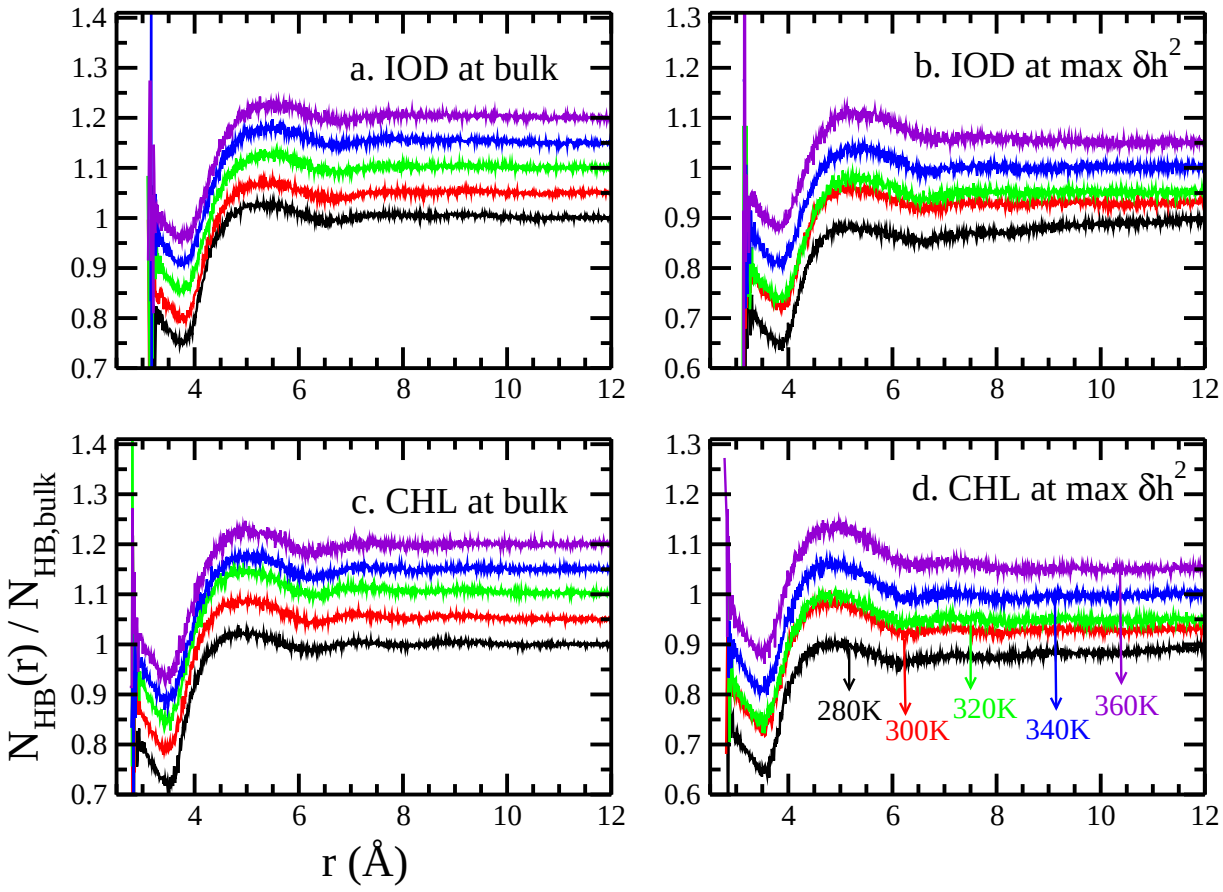

FIG. 16: Normalized number of hydrogen bonds per water molecule as a function of r using the sampling of only the water molecules above I^- when the anion is restrained (a) in the bulk (z = 10 Å) and (b) at the window with largest fluctuations. Panel (c) and (d) show the corresponding normalized hydrogen profiles for Cl^-.

The dipole moment profiles of TIP4P-FQ near the anions are also studied as functions of r. The dipole moment of

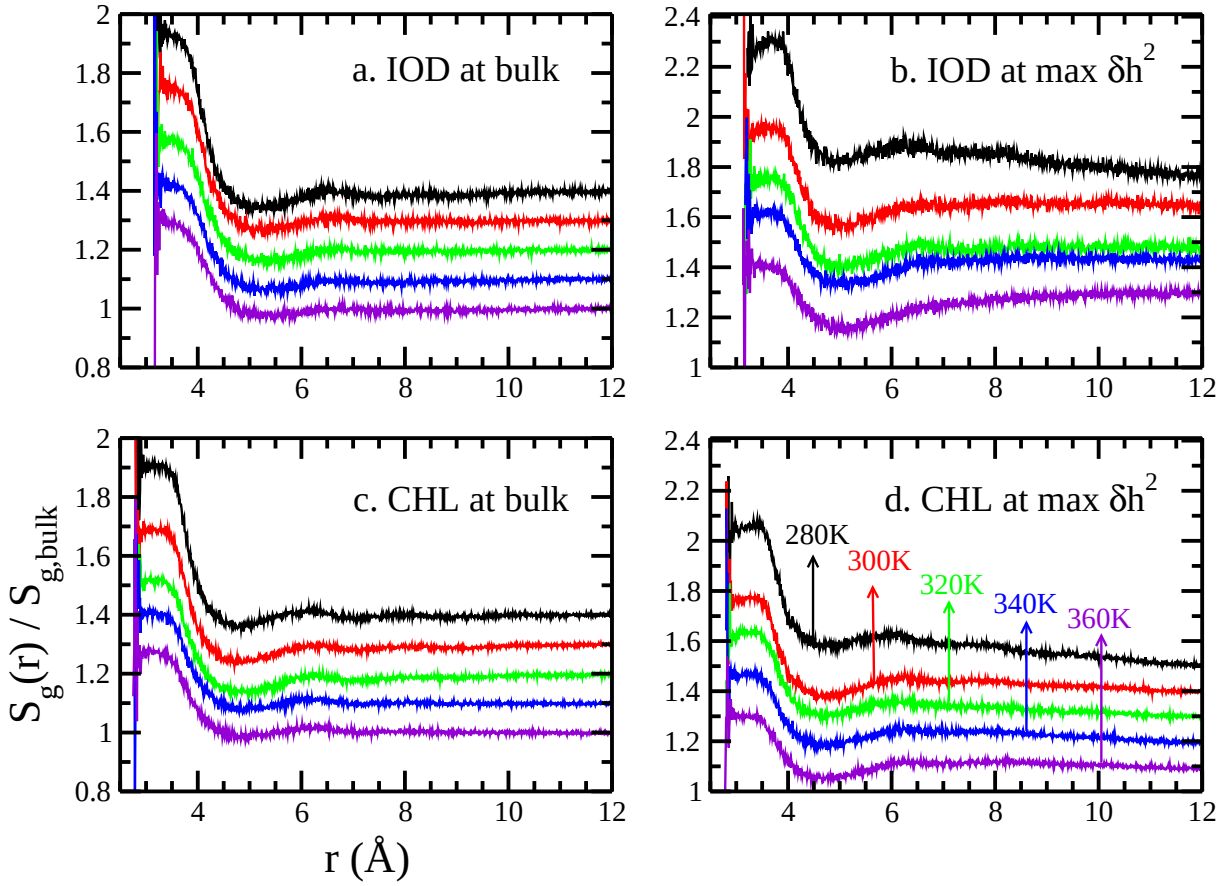

FIG. 17: Normalized Tetrahedral parameter as a function of r using the sampling of only the water molecules above I^- when the anion is restrained (a) in the bulk ($z = 10$ Å) and (b) at the window with largest fluctuations. Panel (c) and (d) show the corresponding normalized tetrahedral profiles for Cl^-. A vertical offset of 0.05 is added for clarity.

a water is computed by

$$\vec{\mu} = \sum_i \vec{r_i} q_i \tag{4}$$

$\langle \mu(r) \rangle$ is then the average of the magnitude of $\vec{\mu}$, as shown in Figure 18. The dipole moment of water in the very vicinity of both ions show increment, with stronger effect near Cl^-. As the ion approaches the L-V interface, $\langle \mu(r) \rangle$ starts to reduce. A vertical offset of 0.1 is added for clarity.

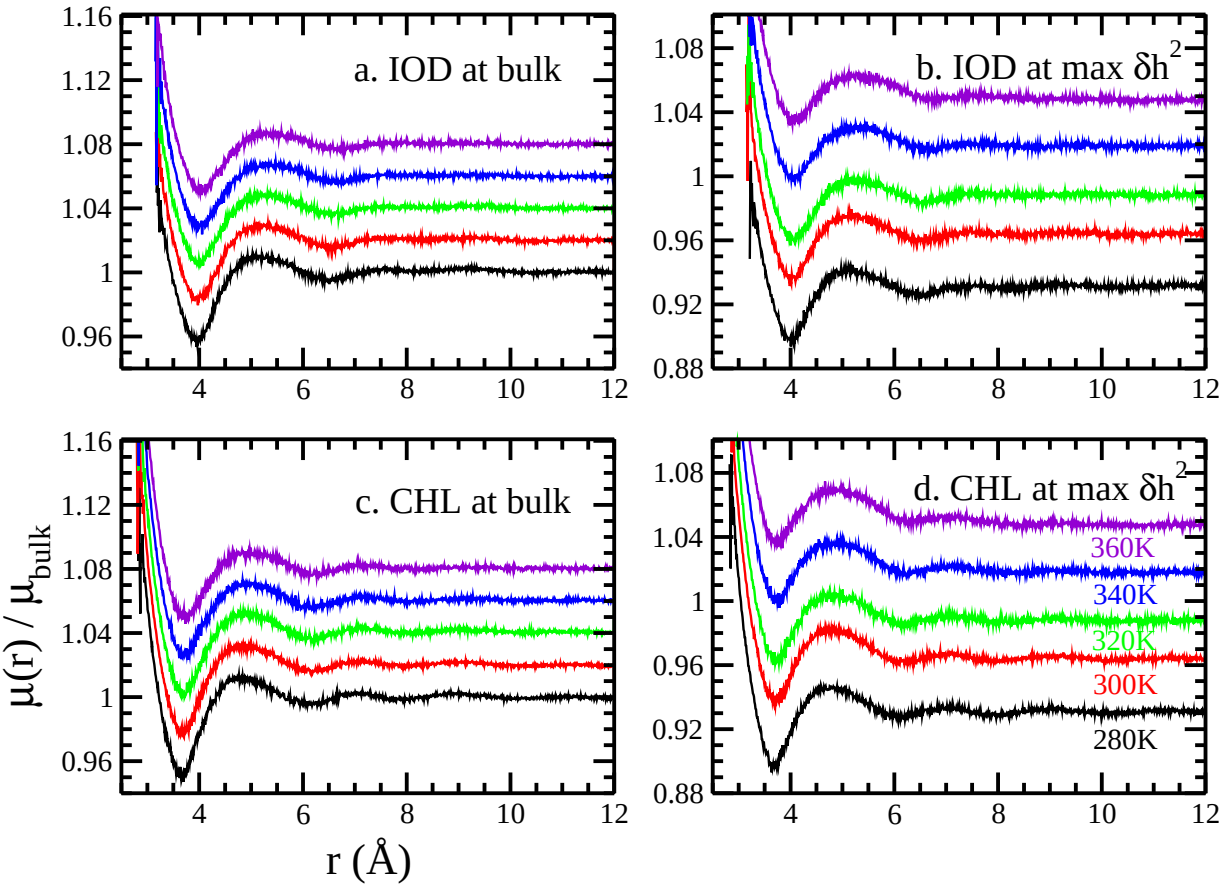

FIG. 18: Normalized dipole moment as a function of r using the sampling of only the water molecules above I^- when the anion is restrained (a) in the bulk (z = 10 Å) and (b) at the window with largest fluctuations. Panel (c) and (d) show the corresponding normalized dipole moment profiles for Cl^-. A vertical offset of 0.02 is added for clarity.

[1] Zhu, F.; Hummer, G. Convergence and Error Estimation in Free Energy Calculations Using the Weighted Histogram Analysis Method. *J. Comp. Chem.* **2012**, *33*, 453–465.

[2] Flyvbjerg, H.; Petersen, H. G. Error Estimates on Averages of Correlated Data. *J. Chem. Phys.* **1989**, *91*, 461–466.

[3] Bauer, B. A.; Ou, S.; Patel, S. Solvation Structure and Energetics of Single Ions at the Aqueous Liquid-Vapor Interface. *Chem. Phys. Lett.* **2011**, *527*, 22–26.

[4] Liu, P.; Harder, E.; Berne, B. J. Hydrogen-Bond Dynamics in the Air-Water Interface. *J. Phys. Chem. B* **2005**, *109*, 2949–2955.

[5] Chau, P.-L.; Hardwick, A. J. A new order parameter for tetrahedral configurations. *Mol. Phys.* **1998**, *93*, 511–518.